Remote Acoustic Imaging of Geosynchronous Satellites

Zachary Watson,[1] Michael Hart
College of Optical Sciences, University of Arizona,1630 E. University Blvd., Tucson, AZ 85721

Abstract

Identification and characterization of orbiting objects that are not spatially resolved are challenging problems for traditional remote sensing methods. Hyper temporal imaging, enabled by fast, low-noise electro-optical detectors is a new sensing modality which may allow the direct detection of acoustic resonances on satellites enabling a new regime of signature and state detection. Detectable signatures may be caused by the oscillations of solar panels, high-gain antennae, or other on-board subsystems driven by thermal gradients, fluctuations in solar radiation pressure, worn reaction wheels, or orbit maneuvers. Herein we present the first hyper-temporal observations of geosynchronous satellites. Data were collected at the Kuiper 1.54-meter telescope in Arizona using an experimental dual-channel imaging instrument that simultaneously measures light in two orthogonally polarized beams at sampling rates extending up to 1 kHz. In these observations, we see evidence of acoustic resonances in the polarization state of satellites. The technique is expected to support object identification and characterization of on-board components and to act as a discriminant between active satellites, debris, and passive bodies.

1. Motivation

Our modern reliance on space assets need not be reiterated given their broad span of technical uses and value to the commercial, military, and civil sectors. What should be stated are the practical challenges of identifying, maintaining, and characterizing the growing population of unresolved objects in geosynchronous orbits (GEO). The challenge presented by GEO objects is that given their distance from earth at 36,000 kilometers, the satellites, debris, and rocket bodies are unresolvable by traditional means without the use of very expensive sensors with large aperture.

Because these objects are not resolved, essential tasks such as object identification, debris and threat discrimination, on-board activity monitoring, and the detection of close-by objects are non-trivial problems. This is coupled with the reality that these satellites have limited life-spans given the harsh space environment where weathering degrades craft thermal surfaces and the wearing of mechanical features can lead to critical component failure [1]. Improved characterization and prediction may lead to mitigation strategies in the event of imminent on-orbit failure as happened with the AMC-9 communications satellite which experienced orbit anomalies in mid-June 2017 and subsequently fragmented into several pieces of debris [2]. The problems further associated with GEO are human in origin and include satellite cross-tagging and the inability to meaningfully defend against artificial threats which can seriously impact national security and warfighter operations. Given these operational and physical challenges, technologies that can provide early threat warning and orbital assessment are critical to maintaining on-orbit capabilities.

Standard astrometry, photometry, and spectroscopy have limitations when addressing the observational needs of satellite operators. There is therefore room for the development of new sensing modalities capable of creating unique signatures without the need to explicitly resolve objects and which ideally may be fielded on both ground- and space-based platforms. Hyper-temporal imaging, a method for remote sensing of acoustic vibrations, is one such technique [3].

2. Methodology

The novel approach we take to satellite signatures is through acoustic or hyper-temporal imaging as it is referred to herein. The basis of this technique is to optically detect weak and rapid oscillations in the intensity of the satellite on the principle that the observed specular reflections fluctuate as a result of movements of semi-rigid modulating mechanical surfaces. By optically sampling these fluctuations at appropriate rates, chirps and resonant vibrations

[1] Now with Hart Scientific Consulting International LLC.

indicative of on-board activity can be captured in the time-series photometry of an object. In practice, the expected drivers of these acoustic oscillations are the movement of appendages such as solar panels and high-gain antennae as perturbed by a range of forces, for example solar radiation pressure, thermal gradients, worn reaction wheels, and thruster firing.

We have made acoustic measurements of a number of GEO satellites using a new prototype instrument attached to the 1.54-m Kuiper telescope of the University of Arizona. We anticipate a problem, however, when viewing an unresolved source through the atmosphere: the total intensity is subject to scintillation that will mask any acoustic signature. Our instrument therefore implements a modification of previous work in remote acoustic sensing. Rather than relying on the total intensity, we synchronously measure the intensities in two orthogonal polarizations separately. We can then calculate the change in the degree of polarization. This technique relies for its utility on the fact that a non-metallic surface imparts a change in the polarization of incident light on reflection which depends on the angle of incidence. The largest reflectors on a satellite are generally the solar panels, which present largely non-metallic surfaces, so it is expected that any acoustic oscillations will induce change in both the angle and degree of polarized light reflected. Propagation through the atmosphere can be treated by Mie scattering theory where the propagation is predominantly in the forward direction, and the initial polarization is preserved [4]. In practice, the differential measurement of the two polarization states acts a natural common-mode rejection filter for active noise sources such as scintillation, large variations in received intensity, or telescope pointing error.

To physically measure changes in the degree of linear polarization (DOLP), we independently and simultaneously measure the orthogonal polarization states as separated by a linear polarizer. In this modality, we are not distinctly measuring any of the Stokes parameters as Q, U, or V but rather just the change in the DOLP as a function of time. This measurement problem is illustrated below in Figure 1.

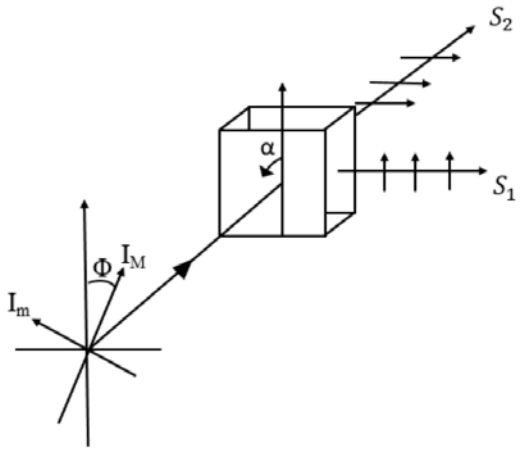

Figure 1. Illustrated is the linear polarization incident upon a polarizing cube beam splitter. In this illustration the resultant and detected orthogonally polarized signals are S_1 and S_2.

As the signal propagates, originating from the specular surface reflection, and passes through the collecting optics towards the downstream linear polarizer, the two resultant orthogonal signals are defined as S_1 and S_2 and respectively written as equations 1 and 2.

$$S_1(\alpha) = T(t)G_1\{I_M cos^2(\alpha + \phi) + I_m sin^2(\alpha + \phi)\} + \eta_1 \quad \text{eq. 1}$$

$$S_2(\alpha) = T(t)G_2\{I_M sin^2(\alpha + \phi) + I_m cos^2(\alpha + \phi)\} + \eta_2 \quad \text{eq. 2}$$

The signals S_1 and S_2 are dependent on the angle α at which the polarizer meets the optical axis. The optical beams are sullied by the common atmospheric and transparency term $T(t)$, and the individual intrinsic detector noise is written as η_1 and η_2. The gain factors for each detected beam are denoted by G_1 and G_2, the maximum and minimum intensity

factors of the observed partially polarized source are written as I_M and I_m, and ϕ is the angle which the direction of I_M makes with the defined axis. The DOLP $\mathcal{P}$ is then written as equation 3 [5].

$$\mathcal{P}(t) = \frac{S_2 - S_1}{S_2 + S_1} \qquad \text{eq. 3}$$

All further analysis relies on this time-series measurement alone.

3. Observations and Instrumentation

Observations were recorded at the 1.54-m telescope in early January 2017. Measurements were made using an experimental dual-channel imager consisting of two separate but identical sCMOS detectors with attached hardware for image synchronization. In operation, each detector simultaneously images the S and P linear polarizations onto a limited field of view as separated by a polarizing beam cube splitter. The optical layout is shown below in Figure 2.

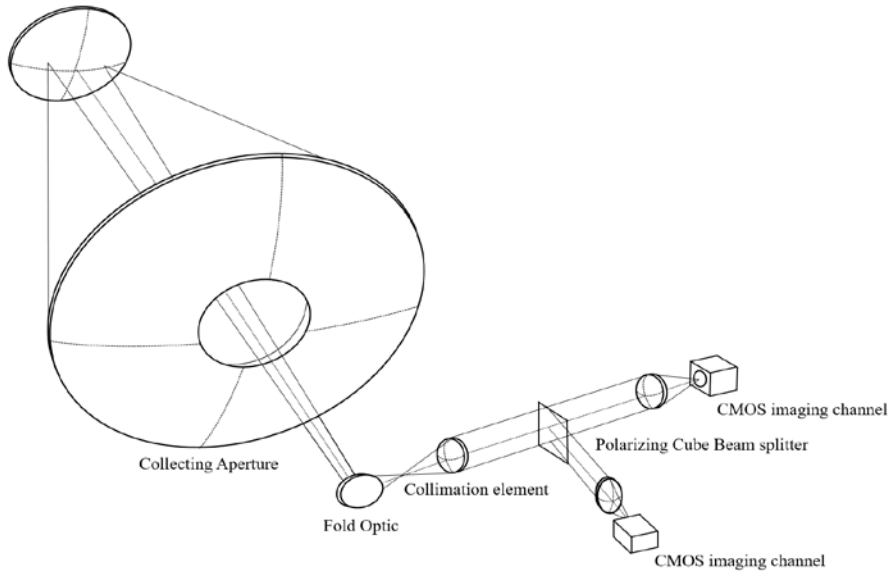

Figure 2. Schematic for the optical train of the hyper-temporal imaging instrument.

As illustrated, the reflected light of the satellite is collected by the telescope where our downstream instrument reimages the separate orthogonal linear polarizations at the appropriate platescale and in practice at sampling rates up to 1 kHz with intrinsic object brightness being the limiting factor. Each detector was independently verified to have read noise below 2 e^- rms and in addition independent laboratory test using pulse tones verified that our experimental instrument and techniques were capable of sensing the predicted acoustic oscillations.

Many observations were made of GEO satellites AMC-16, Anik F1R, and Star One B4, and for control sets several stellar sources of varying magnitude and elevation. We present analysis of two communications satellites, AMC-16 (28472) and Star One B4 (Brasilsat B4, 26469), representing a range in that data covering separate targets, object visual magnitudes, instrument sampling rates, and temporally separated observations. During the January run, AMC-16 was observed at an imaging cadence of 100 Hz during which time it appeared at visual magnitude of approximately $M_v = 11$. Star One B4 was caught during an extended glint, appearing at $M_v = 9.3$, which allowed us to observe it at an imaging cadence of 938 Hz. The run in September was hampered by poor weather and clouds, so observations were obtained only on AMC-16, and at reduced frame rate of 10 Hz.

Cartoons of the two satellites, which have very different architectures, are shown in Figure 3. The AMC-16 satellite is built around a Lockheed Martin A2100AXS bus and represents an extended solar panel architecture with expected oscillations from their resonant movement. The Star One B4 satellite is built around a Boeing HS-376W architecture

representing a cylindrical barrel body which we expect to exhibit little acoustic activity. However the large actively despun antenna we believe will drive any on-board acoustics.

Figure 3. Cartoons of the Lockheed Martin A2100AXS (left) and the Boeing HS-376W (right) which typify AMC-16 and Star One B4 respectively.

4. Results and Analysis

The first step in the analysis is illustrated in Figure 4 which shows sample data streams of the normalized DOLP and the two imaging channel photometry streams representing the separate orthogonal linear polarization states. No useful information is apparent by simple visual inspection of any of the three separate data streams. The two raw photometry streams show common-mode effects of atmospheric scintillation and the slowly changing solar phase angle more strongly than any acoustic effects of the object. Instead, to derive acoustic signatures, we calculate power spectra for

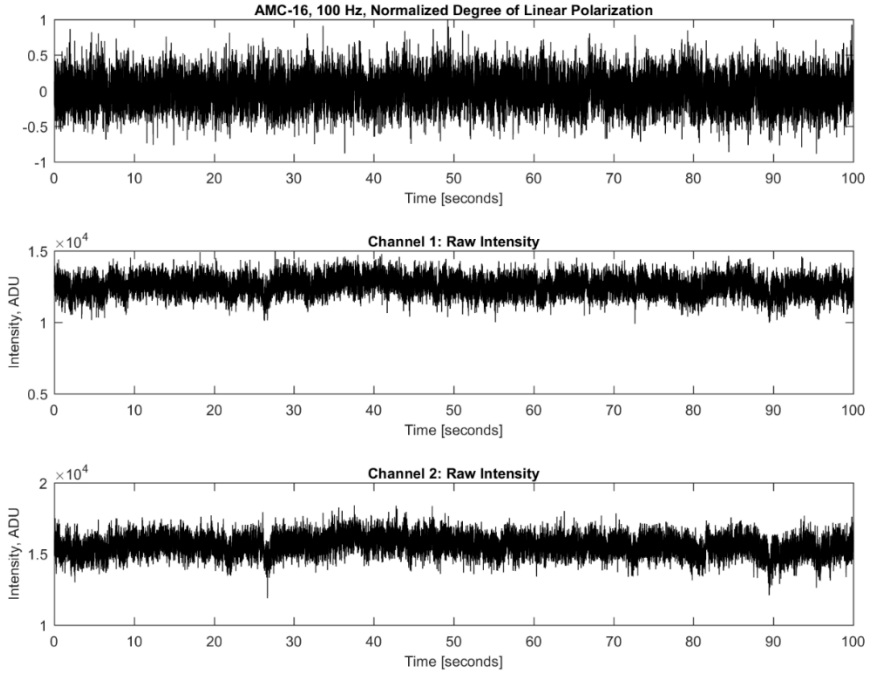

Figures 4. (Top) Normalized time-series DOLP measurement. (Middle and bottom) Raw photometry channels with observed fluctuations attributable to scintillation and changes in solar phase angle. These plots represent 100 seconds of data recorded at an imaging cadence of 100 Hz for AMC-16.

each data stream to reveal any acoustic signal present: peaks in the spectra represent the frequencies of physical resonant vibrations.

A spectrum of the time series DOLP measurements computed from 20,000 frames of data on AMC-16 at 100 Hz is shown in Figure 5. Also shown is the spectrum of a star, η Piscium. At frequencies above a few hertz the satellite and star spectra approach the same level, though the stellar spectrum is less noisy. At magnitude 3.6 it is approximately 1000 times brighter than the satellite. However, at lower frequencies, while the stellar spectrum remains essentially flat and featureless, the satellite spectrum shows evidence of strong acoustic features, with a range of peaks standing out at more than five times the noise observed in the high frequency regions.

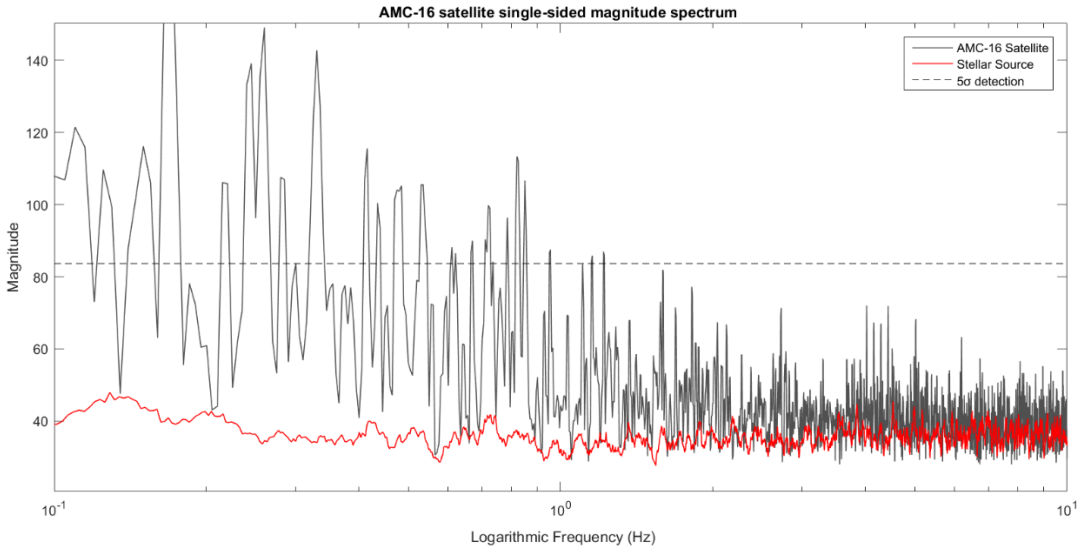

Figure 5. (Black) The acoustic spectrum of the AMC-16 satellite from DOLP measurements acquired in January 2017 at a rate of 100 Hz. Overlaid in red-line is the spectrum of a field stellar calibration source.

The difference in low-frequency structure is critical: on the timescales of these experiments stellar sources do not intrinsically oscillate in brightness or polarization with any appreciable amplitude. There is an important difference also in the data collections, however: the satellite is by design almost stationary with respect to the telescope while the star moves at the sidereal rate. To avoid any artifacts attributable to resonances in the telescope, we therefore kept the drive motors on during the satellite data collection even though the tracking motion was extremely small and did not require them. The distinction in the spectra is therefore strong evidence that we are sensitive to acoustic resonances on board the satellite. The lack of structure in the stellar source confirms that the features we see in the satellite spectrum are not an instrumental effect or effect of pointing error. The oscillations represent brightness changes in each polarization channel of approximately 0.5%.

We have also explored the data for evidence of variability in spectral structure with time. Spectrograms as a function of time have been computed for AMC-16, Star One B4, and the asteroid Vesta, representing a natural calibrator object. The spectrograms are computed as the power spectra of successive short sequences of the DOLP time series, with each sequence overlapping the previous one by 50%. In this way, changes in the spectral content of the DOLP signal can be revealed.

The results for the three objects are shown in Figure 6. Consistent with the spectrum of Figure 5, the AMC-16 spectrogram is characterized by power at the lowest frequencies, below 1 Hz, with randomly varying noise at higher frequencies. There is some evidence that the low-frequency signal is varying on time scales of roughly 20 s, but this needs further investigation. The spectrogram of Star One B4 shows a distinctly different character with a broad band of power in frequencies below 100 Hz that lasts for approximately 10 s. (A second observation of the satellite shows a similar phenomenon.) Finally, the spectrogram of Vesta shows nothing but noise, with no regions of significant power. This is encouraging, since again, we do not expect the natural object to display any significant spectral features.

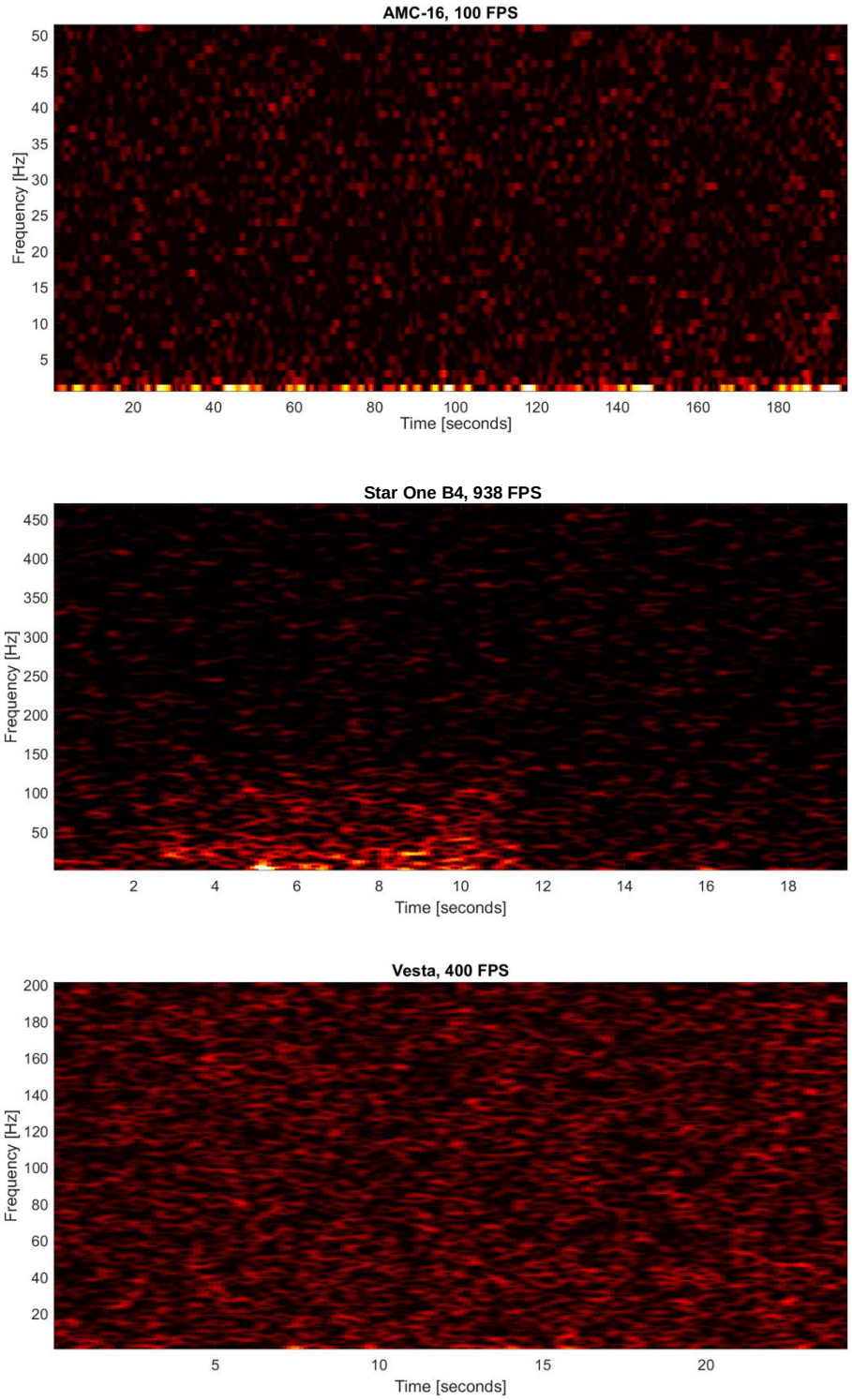

Figure 6. Spectrograms of (top to bottom) AMC-16 at 100 fps; Star One B4 at 938 fps; Vesta at 400 fps. The vertical scale in these plots is arbitrary and not the same in each case.

5. Conclusion

Our novel technology demonstration of hyper-temporal imaging shows evidence for acoustic oscillations present on observed GEO targets while our control data of astronomical sources show no such acoustic features. It is tempting to believe that the spectral features we see originate in the movement of the solar panels on-board the AMC-16 satellite and from the despun high-gain antenna on the Star One B4 satellite. As yet, however, we have no independent corroboration of that hypothesis.

We observe these acoustic oscillations in the change in the degree of linear polarization rather than the high-speed raw photometry measurements which are strongly affected by atmospheric noise. Given this evidence that on-board mechanical activity may be remotely monitored, hyper-temporal imaging presents itself as a new sensing modality with which qualitatively new information about the population of non-resolved objects on orbit can be acquired.

6. Acknowledgments

Many thanks are owed to the Mountain Operations team of Steward Observatory for their continued technical support and assistance and to T.G. Smith and K.A. Pearson for observing assistance. The hyper-temporal imaging instrument was funded by the University of Arizona's Technology Research Initiative Fund.

7. References

[1] Jorgensen, K., Okada, J., Guyote, M., Africano, J., Hall, D., Hamada, K., Barker, E., Stansbery, G., and Kervin, P., Reflectance Spectra of Human-made Objects, 2004 AMOS Technical Conference, Wailea, Maui, Hawaii, 8 – 12 September 2004.

[2] Space Intel Report. Peter B. de Selding. July 02, 2017. SES re-establishes communications with AMC-9; pieces of satellite appear to have broken off. Online at: https://www.spaceintelreport.com/ses-re-establishes-communications-amc-9-pieces-satellite-appear-broken-off/

[3] Slater, D., Kozacik, S., and Kelmelis, E., "Photo-acoustic and video-acoustic methods for sensing distant sound sources," Long-Range Imaging II (Proc. SPIE), 10204, 1020408, 2017.

[4] Schott, J., "Fundamentals of Polarimetric Remote Sensing," SPIE Press, Bellingham Washington. 2009

[5] Clarke, D., "Theoretical Considerations in the Design of an Astronomical Polarimeter," MRNAS, Vol. 129, p.71-84, 1964.